Bull. Chem. Soc. Jpn., 71, 119—125 (1998)

Structure and Magnetic Properties of a Chain Complex with Alternating Ru(II,III) Dimer and Nitroxide Radical Arrangement $[Ru_2(O_2CCMe_3)_4(nitph)]_n(BF_4)_n$, nitph = 2-Phenyl-4,4,5,5-tetramethyl-4,5-dihydro-1*H*-imidazol-1-oxyl 3-*N*-Oxide

Makoto Handa,* Yasuyoshi Sayama,† Masahiro Mikuriya,*,† Ryoji Nukada,† Ichiro Hiromitsu, and Kuninobu Kasuga

Department of Material Science, Interdisciplinary Faculty of Science and Engineering, Shimane University, Nishikawatsu, Matsue 690

†Department of Chemistry, School of Science, Kwansei Gakuin University, Uegahara, Nishinomiya 662

(Received April 24, 1997)

A chain complex of diruthenium(II,III) cation dimer linked by a nitroxide radical, $[Ru_2(O_2CCMe_3)_4(nitph)]_n(BF_4)_n$ (nitph = 2-phenyl-4,4,5,5-tetramethyl-4,5-dihydro-1*H*-imidazol-1-oxyl 3-*N*-oxide), has been prepared and characterized. The structure with an alternating alignment of Ru(II,III) core and nitph has been confirmed by the X-ray crystal analysis. The magnetic moment decreased steadily with decrease of temperature, against the expectation of ferrimagnetic behavior based on the alternated alignment of $S_1 = 3/2$ (for Ru(II,III) core) and $S_2 = 1/2$ (for nitph). It has been found that the zero-field splitting plays an important role in the magnetic behavior in addition to the interaction between the Ru(II,III) core and nitph.

Recently, many types of polymers of transition metal complexes linked by bridging ligands have been prepared.[1—6] Some of them have shown interesting physicochemical properties. In order to obtain such properties, the combination of metal complexes and ligands must be carefully chosen.

We have been engaged in the preparation of the polymers constructed by $M_2(O_2CR)_4^{0/+}$ (M=Cu, Mo, Ru, and Rh) and bidentate ligands.[7] Among the M_2 dimers, Ru(II,III) dimer has more than one unpaired electron in the degenerate orbitals ($\sigma^2\pi^4\delta^2(\pi^*\delta^*)^3$). This attracted our interest to use the dimer as a unit bridged by the ligand to produce paramagnetic polymers. Such studies have been made on the chain complexes of $Ru_2(O_2CR)_4^+$ (R = Me and Et) bridged by phenazine and pyrazine.[2] We have initiated a research project concerning the polymer complexes of $Ru_2(O_2CR)_4^+$ bridged by nitroxide radicals with the expectation that the polymers would give the ferrimagnetic properties[3,8] which originate from the alternated [$S = 3/2$ (Ru(II,III) dimer)] – [$S = 1/2$ (nitroxide radical)] alignment. The fairly strong antiferromagnetic interaction between a Ru_2 cation and a nitroxide radical has been already confirmed for the complex $[Ru_2(O_2CCMe_3)_4(tempo)_2][Ru_2(O_2CCMe_3)_4(H_2O)_2](BF_4)_2$ (tempo=2,2,6,6-tetramethylpiperidine-1-oxyl) (**1**).[9] Here, we present crystal structure and magnetic properties of a chain complex $[Ru_2(O_2CCMe_3)_4(nitph)]_n(BF_4)_n$ (nitph=2-phenyl-4,4,5,5-tetramethyl-4,5-dihydro-1*H*-imidazol-1-oxyl 3-*N*-oxide) (**2**). To our knowledge, crystallographically characterized nitroxide adduct complexes of Ru(II,II) or Ru(II,III) dimer have been limited to only two examples: $Ru_2(O_2CCF_3)_4(tempo)_2$[10] and **1**. A preliminary account of this study has been previously reported.[7i]

Experimental

The starting material $[Ru_2(O_2CCMe_3)_4]BF_4$ was prepared by a similar procedure to that described in the literature.[11]

Preparation of $[Ru_2(O_2CCMe_3)_4(nitph)]_n(BF_4)_n$ (2). A benzene solution (5 cm^3) of nitph (8.2 mg, 0.035 mmol) was added to a benzene solution (5 cm^3) of $Ru_2(O_2CCMe_3)_4BF_4$ (19 mg, 0.027 mmol) under argon atmosphere. After the solution was stirred overnight at room temperature, the precipitate was filtered, washed with benzene, and dried by heating at 80 °C under vacuum. Yield: 18.8 mg (75% based on $[Ru_2(O_2CCMe_3)_4]BF_4$). Anal. Found: C, 42.58; H, 5.44; N, 3.00%. Calcd for $C_{33}H_{53}BF_4N_2O_{10}Ru_2$: C, 42.77; H, 5.76; N, 3.02%.

Measurements. Elemental analyses for carbon, hydrogen, and nitrogen were carried out using a Yanako CHN CORDER MT-5. Magnetic susceptibilities were measured by the Faraday method over the 5—300 K temperature range. The apparatus was calibrated using $[Ni(H_2NCH_2CH_2NH_2)_3]S_2O_3$.[12] The susceptibilities were corrected for diamagnetism of the constituent atoms using Pascal's constants.[13]

X-Ray Crystal Structure Analysis. Crystals suitable for a single-crystal X-ray structure determination were obtained from a benzene solution as those with solvated benzene molecules, $[Ru_2(O_2CCMe_3)_4(nitph)]_n(BF_4)_n \cdot 2n$(benzene) (**2**·2*n*(benzene)) by slow diffusion technique using H-shaped tube. The unit-cell parameters and intensities were measured on an Enraf–Nonius CAD-4 diffractometer with graphite-monochromated Mo $K\alpha$ radiation ($\lambda = 0.71073$ Å) at 25±1°C. The intensity data were collected by ω–2θ scan technique and were corrected for Lorentz-polarization

effects and absorption. The transmission factors were in the range 0.96—1.00.

Crystal Data: $Ru_2F_4O_{10}N_2C_{45}BH_{65}$, F.W. = 1082.96, monoclinic, space group $P2_1/n$, a=23.582(8), b=20.528(3), c=11.087(4) Å, β=93.33(2)°, V=5358(3) Å^3, Z=4, D_m=1.35, D_c=1.34 g cm^{-3}, μ(Mo $K\alpha$)=6.14 cm^{-1}, crystal dimensions 0.42×0.25×0.17 mm^3. Of the 8676 reflections measured in the range $2.0 \leq 2\theta \leq 48.0°$, 4106 with $I \geq 3\sigma(I)$ were assumed as observed. The structure was solved by direct methods and refined by full-matrix least-squares method. All non-hydrogen atoms were refined with anisotropic thermal parameters. There are disorders at three carbon atoms on *t*-butyl group of pivalate and hence they are divided into two positions with same weights, respectively. Hydrogen atoms were inserted at their calculated positions and fixed at their positions. A weighting scheme $w = 1/[\sigma^2(|F_o|) + (0.02|F_o|)^2 + 1.0]$ was employed. The final discrepancy factors were $R = \sum||F_o| - |F_c||/\sum|F_o| = 0.061$ and $R_w = [\sum w(|F_o| - |F_c|)^2/\sum|F_o|^2]^{1/2} = 0.069$.

All the calculations were carried out on a Micro-VAX station 4000 (90A) with the MolEN program package.[14] The atomic coordinates and thermal parameters of non-hydrogen atoms are listed in Table 1. The anisotropic thermal parameters of non-hydrogen atoms, the atomic coordinates and temperature factors of hydrogen atoms, and the $F_o - F_c$ tables were deposited as Document No. 70050 at the Office of the Editor of Bull. Chem. Soc. Jpn.

Result and Discussion

The elemental analysis revealed that the complex has a stoichiometry $Ru_2(O_2CCMe_3)_4^+$: nitph : BF_4^- = 1 : 1 : 1 even though excess nitph was used for the reaction. Analysis of the complex before drying by heating under vacuum showed the presence of benzene in the crystal.

In Fig. 1, the crystal structure of **2**·2*n*(benzene) is shown. The $Ru_2(O_2CCMe_3)_4$ unit is axially coordinated by nitph to form a chain structure with an alternating arrangement of the Ru_2 dimer and nitph. Selected bond distances and angles are given in Table 2. The axial Ru–O bond distances are 2.264(8) (for Ru1–O9) and 2.236(8) Å (for Ru2–O10′). These values are a little larger than those of **1** (2.184(3) Å)[9] and $Ru_2(O_2CCF_3)_4(tempo)_2$ (2.136(5) Å (201 K) and 2.162(4) Å (293 K)).[10] The Ru–Ru bond distance of 2.266(1) Å is in

Table 1. Fractional Positional Parameters and Thermal Parameters of Non-Hydrogen Atoms with Their Estimated Standard Deviations in Parentheses

Atom	x	y	z	B_{eq}/Å^2 [a]	Atom	x	y	z	B_{eq}/Å^2 [a]
Rul	0.72008(4)	−0.38803(5)	0.67234(9)	2.63(2)	C14	0.7004(9)	−0.597(1)	0.393(2)	9.3(6)[b]
Ru2	0.75167(5)	−0.48327(4)	0.75481(9)	2.66(2)	C15	0.609(1)	−0.544(1)	0.432(2)	11.8(7)[b]
F1	0.9397(5)	−0.2152(7)	0.428(1)	10.9(4)	C16	0.8342(5)	−0.4200(7)	0.619(1)	3.8(3)
F2	0.9512(5)	−0.1933(8)	0.237(1)	12.7(4)	C17	0.8900(6)	−0.4123(7)	0.556(1)	5.4(4)
F3	0.8758(7)	−0.2387(9)	0.288(2)	18.0(6)	C18	0.8788(9)	−0.408(1)	0.426(2)	9.0(5)[b]
F4	0.8902(7)	−0.1428(8)	0.342(1)	15.1(5)	C19	0.9304(8)	−0.464(1)	0.595(2)	8.4(5)[b]
O1	0.7495(4)	−0.3408(4)	0.8228(7)	3.9(2)	C20	0.917(1)	−0.350(1)	0.606(2)	9.9(6)[b]
O2	0.7801(4)	−0.4350(4)	0.9042(7)	3.7(2)	C21	0.6874(5)	−0.1890(5)	0.676(1)	3.2(3)
O3	0.6446(3)	−0.4032(4)	0.7430(8)	3.7(2)	C22	0.7221(6)	−0.2088(6)	0.485(1)	4.4(3)
O4	0.6756(3)	−0.4964(4)	0.825 1(7)	3.6(2)	C23	0.7546(6)	−0.1483(6)	0.542(1)	3.9(3)
O5	0.6910(4)	−0.4353(4)	0.5226(7)	3.7(2)	C24	0.6551(5)	−0.1935(6)	0.785(1)	3.6(3)
O6	0.7217(4)	−0.5298(4)	0.6039(7)	3.4(2)	C25	0.6701(7)	−0.1584(7)	0.886(1)	5.3(4)
O7	0.7964(4)	−0.3762(4)	0.6013(7)	3.8(2)	C26	0.6392(8)	−0.1608(9)	0.988(1)	6.9(4)
O8	0.8269(3)	−0.4707(4)	0.6818(7)	3.6(2)	C27	0.5905(7)	−0.1973(9)	0.987(2)	8.5(4)
O9	0.6782(4)	−0.2955(4)	0.6006(8)	4.1(2)	C28	0.5735(6)	−0.2318(9)	0.885(2)	7.2(4)
O10	0.7086(4)	−0.0783(4)	0.6891(8)	4.1(2)	C29	0.6059(7)	−0.2309(8)	0.787(2)	6.1(4)
Nl	0.6964(4)	−0.2359(5)	0.5962(9)	3.7(2)	C30	0.7595(7)	−0.2585(7)	0.429(1)	5.8(4)
N2	0.7147(4)	−0.1339(4)	0.6402(9)	3.1(2)	C31	0.6727(8)	−0.1908(8)	0.400(1)	6.7(4)
Cl	0.7742(6)	−0.3734(6)	0.908(1)	3.9(3)	C32	0.8111(6)	−0.1633(8)	0.604(1)	5.2(4)
C2	0.7973(8)	−0.3372(8)	1.021(1)	6.3(4)	C33	0.7564(7)	−0.0915(7)	0.457(1)	5.5(4)
C3a	0.826(1)	−0.273(2)	0.978(3)	6.2(7)[b]	C34	0.523(1)	−0.132(1)	0.430(2)	11.5(8)[b]
C3b	0.863(2)	−0.340(2)	1.014(4)	8(1)[b]	C35	0.524(1)	−0.135(1)	0.541(3)	13.0(9)[b]
C4a	0.833(1)	−0.375(2)	1.102(3)	6.8(8)[b]	C36	0.559(1)	−0.085(1)	0.602(2)	12.3(8)[b]
C4b	0.782(1)	−0.376(2)	1.134(3)	6.6(8)[b]	C37	0.580(1)	−0.041(1)	0.533(2)	11.5(7)[b]
C5a	0.739(2)	−0.315(2)	1.085(4)	8(1)[b]	C38	0.578(1)	−0.038(2)	0.413(3)	14.4(9)[b]
C5b	0.776(2)	−0.273(2)	1.034(3)	7.8(9)[b]	C39	0.545(1)	−0.092(2)	0.347(3)	14.2(9)[b]
C6	0.6375(5)	−0.4544(6)	0.805(1)	3.3(3)	C40	1.0632(9)	−0.160(1)	−0.107(2)	9.4(6)[b]
C7	0.5784(6)	−0.4656(7)	0.854(1)	5.3(4)	C41	1.053(1)	−0.172(1)	−0.237(2)	9.9(6)[b]
C8	0.574(1)	−0.525(1)	0.919(3)	13.4(8)[b]	C42	1.0001(9)	−0.188(1)	−0.276(2)	8.5(5)[b]
C9	0.572(2)	−0.415(2)	0.947(4)	19(1)[b]	C43	0.9592(9)	−0.195(1)	−0.197(2)	9.3(6)[b]
C10	0.535(1)	−0.449(2)	0.768(3)	15(1)[b]	C44	0.970(1)	−0.186(1)	−0.080(2)	11.2(7)[b]
C11	0.6959(5)	−0.4984(6)	0.520(1)	3.4(3)	C45	1.0202(9)	−0.170(1)	−0.038(2)	9.5(6)[b]
C12	0.6707(6)	−0.5343(7)	0.412(1)	4.7(3)	B	0.9173(8)	−0.200(1)	0.321(2)	5.8(5)
C13	0.6722(9)	−0.495(1)	0.300(2)	8.8(5)[b]					

a) Anisotropically refined atoms are given in the form of the isotropic equivalent displacement parameter defined as: $(4/3)[a^2B(1,1) + b^2B(2,2) + c^2B(3,3) + ab(\cos\gamma)B(1,2) + ac(\cos\beta)B(1,3) + bc(\cos\alpha)B(2,3)]$. b) Atoms were refined isotropically.

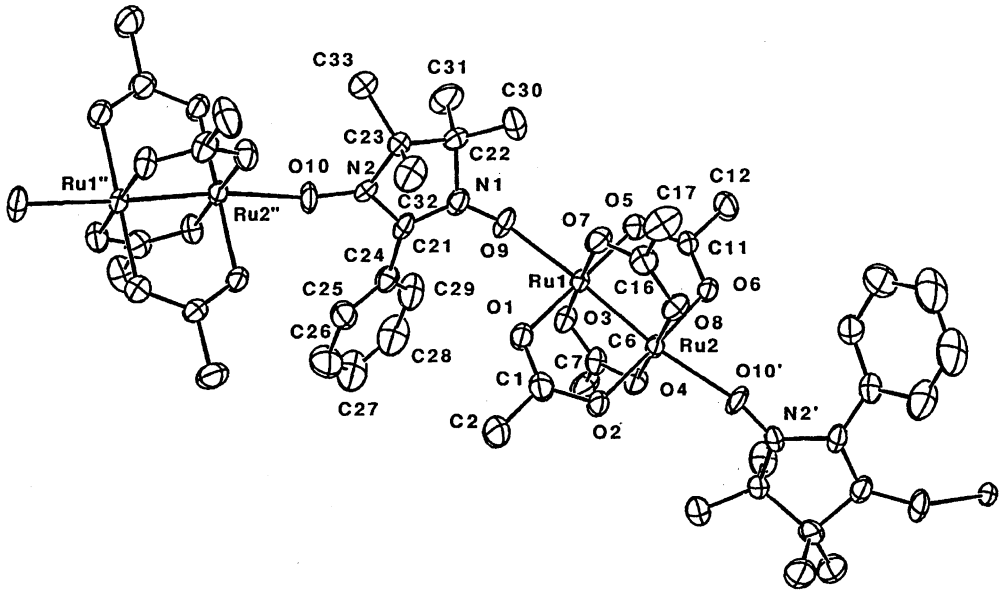

Fig. 1. ORTEP view of $[Ru_2(O_2CCMe_3)_4(nitph)]_n(BF_4)_n \cdot 2n$(benzene) (**2**·2*n*(benzene)). Me groups of the pivalate ions, BF_4^- ions, and benzene molecules are omitted for clarity. Primes and double primes refer to the equivalent positions $(3/2-x, -1/2+y, 3/2-z)$ and $(3/2-x, 1/2+y, 3/2-z)$, respectively.

Table 2. Selected Bond Distances (Å) and Angles (°) of **2**·2*n*(benzene)[a]

Ru1–Ru2	2.266(1)	Ru2–O8	2.010(8)
Ru1–O1	2.017(8)	Ru2–O10′	2.236(8)
Ru1–O3	2.011(8)	O9–N1	1.30(1)
Ru1–O5	2.009(8)	O10–N2	1.28(1)
Ru1–O7	2.020(8)		
Ru1–O9	2.264(8)	Ru2–Ru1–O9	172.9(2)
Ru2–O2	2.012(8)	Ru1–Ru2–O10′	170.9(2)
Ru2–O4	2.015(8)	Ru1–O9–N1	131.7(7)
Ru2–O6	2.018(7)	Ru2–O10′–N2′	147.5(7)

a) Prime refers to the equivalent position $(3/2-x, -1/2+y, 3/2-z)$.

the range of those reported for $[Ru_2(O_2CR)_4]^+$ compounds (2.24—2.30 Å).[15] The N–O bond lengths 1.30(1) and 1.28(1) Å show that the ligand nitph exists as a free radical.[16,17] The Ru–O–N angles are 131.7(7)° for Ru1–O9–N1 and 147.5(7)° for Ru2–O10′–N2′, being different from each other. The Ru2–O10′–N2′ bond angle is close to the Ru–O–N angle values of **1** (151.5(3)°) and $Ru_2(O_2CCF_3)_4(tempo)_2$ (158.2(3)° (201 K) and 157.9(3)° (293 K)). As seen from the packing view of **2**·2*n*(benzene) (Fig. 2), BF_4^- ions and benzene molecules are located between the chains so as to allow no significant contact between the chains.

In Fig. 3, the variations of effective magnetic moments per Ru(II,III) dimer with temperature (5—300 K) for **2**·2*n*(benzene) and $[Ru_2(O_2CCMe_3)_4]BF_4 \cdot 2H_2O$ are shown. The magnetic moments for **2**·2*n*(benzene) are considerably lower than those for $[Ru_2(O_2CCMe_3)_4]BF_4 \cdot 2H_2O$ in the whole temperature range, which shows the existence of an antiferromagnetic interaction between the dimetal center and the radical. The magnetic moment is steadily decreased with lowering of temperature. This behavior is against our expectation. The chain with the alternated arrangement of paramagnetic centers having different spin states ($S=3/2$ (Ru(II,III) core) and $S=1/2$ (nitph)) must show ferrimagnetic behavior when the antiferromagnetic interaction is operative between

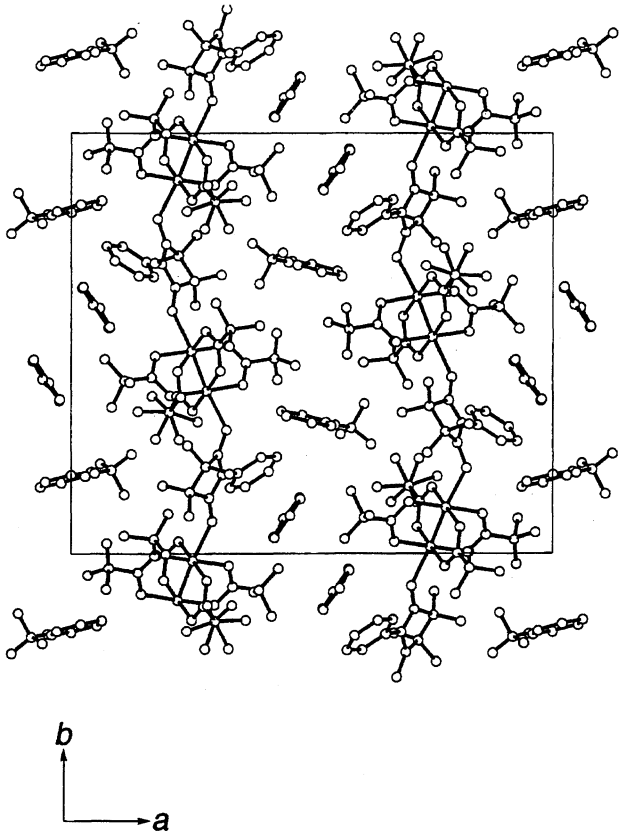

Fig. 2. Perspective view on *ab* plane of **2**·2*n*(benzene). The disordered carbon atoms on *t*-butyl groups are all depicted.

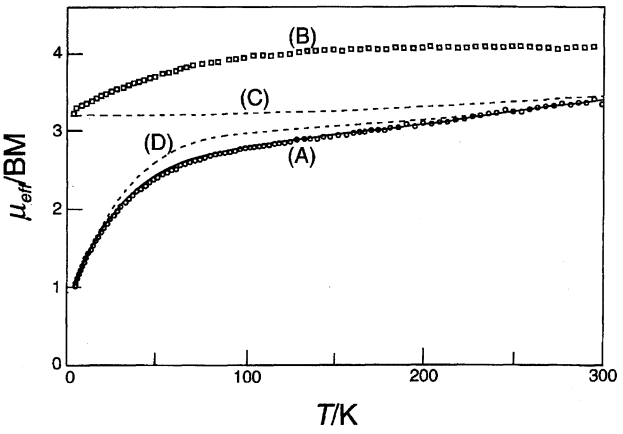

Fig. 3. Temperature dependence of magnetic moments per Ru(II,III) units for **2**·2*n*(benzene) (A) and $Ru_2(O_2CCMe_3)_4BF_4 \cdot 2H_2O$ (B). The solid line was calculated with parameters listed in Table 3. The dashed line (C) is drawn by the equation based on the alternating ferrimagnetic chain model of $S_1 = 3/2$ and $S_2 = 1/2$ without zero-field splitting term, the parameters being set at $g_1 = g_2 = 2.00$, $J = -120$ cm^{-1}, and $\alpha = 1$. The dashed line (D) is drawn by the equation based on the molecular field approximation for the coupled $(S_1 = 3/2) - (S_2 = 1/2)$ unit, the parameters being set at $g_1 = g_2 = 2.00$, $z = 2$, $J = -120$ cm^{-1}, $J' = 5$ cm^{-1}, $D = 80$ cm^{-1}, and $P = 0.045$ (fraction of impurity of ligand-free Ru(II,III) dimer).

the paramagnetic centers.

In order to interpret the magnetic behavior, we used the theoretical equation based on the alternating ferrimagnetic chain model of $S_1 = 3/2$ and $S_2 = 1/2$ without zero-field splitting term[18] for the analysis. However, we could not reach the satisfied result; the continuous decrease of the magnetic moment at temperatures close to 0 K could not be simulated by the equation as exemplified by the dashed line of Fig. 3(C). The theoretical equation derived from the spin Hamiltonian with consideration of zero-field splitting must be employed for the analysis. Unfortunately, the quantitative treatment based on the Hamiltonian is practically impossible because the eigenvalue problem becomes too complicated due to the introduction of the zero-field splitting term.

To simplify the problem, we applied the spin pair model shown below for the present case (See Appendix and Scheme 1). As seen in Fig. 3(A), the cryomagnetic behavior of **2**·2*n*(benzene) can be well simulated using magnetic parameters given in Table 3 where J is the spin coupling constant defined in Scheme 1, and g_{Ru} and g_{nit} are the g factors of the Ru(II,III) core and the nitroxide ligand, respectively, D is the zero-field splitting within the dimetal fragment, and P is the fraction of impurity of ligand-free Ru(II,III) dimer. In the fitting, the g_{Ru} and g_{nit} values were set to 2.00. The D value is comparable to those for $Ru_2(O_2CR)_4^+$ complexes.[2b,9,19]

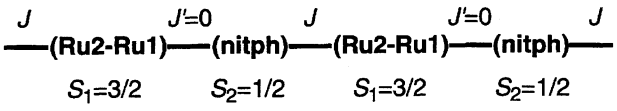

Scheme 1.

Table 3. Fitting Parameters for the Magnetic Data

g_{Ru}	2.00
g_{nit}	2.00
J/cm^{-1}	−100
D/cm^{-1}	65
P	0.045
$R/10^4$ a)	6.23

a) $R = \sum(\chi_{obsd} - \chi_{calcd})^2 / \sum(\chi_{obsd})^2$, where χ is the magnetic susceptibility.

The validity of the analysis was evaluated by looking into the bonding features around the axial sites of the Ru(II,III) dimer. In Table 4, the bonding features and J values for **2**·2*n*(benzene) and the other axially O-bonded nitroxide complexes of $M_2(O_2CR)_4^{0/+}$ (M = Ru and Rh) reported so far are summarized.[4,9,10,20] In the case of **1** and $Ru_2(O_2CCF_3)_4(tempo)_2$, the interaction was interpreted with the mechanism of the pathway based on the π^* orbitals of the N–O group of the nitroxide and diruthenium core judging from their Ru–O–N bond angles, 151.5(3)—158.2(3)°.[9,10] In the case of the rhodium complexes, it has been considered that a Rh–O–N bond angle close to 120° was suited for the interaction between the radical spins through the Rh–Rh bond with the σ-pathway mechanism.[4] The Ru2–O10′–N2′ bond angle of **2**·2*n*(benzene) 147.5(7)° is comparable to the Ru–O–N bond angles of the ruthenium complexes **1** and $Ru_2(O_2CCF_3)_4(tempo)_2$, which may lead to an appreciable antiferromagnetic interaction between the Ru_2 core and the radical. The J value (= −100 cm^{-1}) is comparable to that of **1** (−130 cm^{-1}). On the other hand, the Ru1–O9–N1 bond angle 131.7(7)° is not appropriate for the interaction between the Ru_2 core and the radical with π-pathway mechanism. In addition, the axial Ru1–O9 distance (2.264(8) Å) is longer compared with the Ru2–O10′ distance (2.236(8) Å), which is also unfavorable for the interaction at the Ru1 side. These structural factors may cut down significantly the antiferromagnetic interaction between the Ru_2 core and the radical at the Ru1 side. The Ru1–O9–N1 bond angle could be rather suitable for the interaction between the radicals through the Ru–Ru bond with the σ-pathway mechanism. However, the interaction is considered to be weak because at the other side of the ruthenium dimer (i.e., at the Ru2 side), the σ-pathway mechanism is not favorable.

Cogne et al. performed a quantitative comparison of J values between nitroxide complexes of Rh_2 dimer based on the fact that the antiferromagnetic interaction is proportional to $-\mathscr{S}^2$, where $\mathscr{S}$ is the overlap integral between the magnetic orbitals.[4b] We calculated the $\mathscr{S}$ values between the π^* orbitals of the Ru_2 core[21] and the π^* orbital of the nitroxide radical at the Ru1 and Ru2 sides of **2**·2*n*(benzene) according to their calculating procedure.[4b] The result including the parameters used in the calculation is shown in Table 5 and Fig. 4. The value $(\mathscr{S}_{Ru2}/\mathscr{S}_{Ru1})^2 = 2.95$ means that the antiferromagnetic interaction at the Ru1 side is about 1/3 as large as that at the Ru2 side. The J value (−100 cm^{-1}) at the Ru2 side obtained from spin pair model is expected to remain almost

Table 4. Bonding Parameters and J Values for the Axially O-Bonded Nitroxide Complexes of $M_2(O_2CR)_4^{0/+}$ (M = Ru and Rh)

Compound	M–O_{ax}/Å	M–O_{ax}–N/°	J/cm^{-1}	Ref.
$Ru_2(O_2CCF_3)_4(tempo)_2$	2.136(5)	158.2(3)	−263[b]	10
1	2.184(3)	151.5(3)	−130[c]	9
2·2*n*(benzene)	2.236(8)	147.5(7)	−100[c]	This work
	2.264(8)	131.7(7)	0	
$Rh_2(O_2CCF_3)_4(nitph)_2$	2.239(3)	122.7(3)	−83.6[d]	4
$[Rh_2(O_2CCF_3)_4(nitme)]_n$ [a]	2.268(5), 2.254(5)	118.3(4), 121.3(4)	−98.8[d]	4
$Rh_2(O_2CCF_3)_4(tempo)_2$	2.220(2)	138.0(1)	−239[d]	20
$Rh_2(O_2CC_3F_7)_4(tempo)_2$	2.235(5)	134.2(4)	−269[d]	20

a) nitme = 2,4,4,5,5-pentamethyl-4,5-dihydro-1*H*-imidazol-1-oxyl 3-*N*-oxide. b) J for the interaction between the Ru(II,II) center and the radical. c) J for the interaction between the Ru(II,III) center and the radical. d) J for the interaction between the radicals through the Rh–Rh bond.

unaltered even if J' at the Ru1 side has a finite value, on condition that the $|J'|$ value at the Ru1 side is substantially lower than the $|J|$ value at the Ru2 side (see Scheme 1). The continuous decrease of magnetic moment of **2**·2*n*(benzene) with decrease of temperature may be associated with the fact that the interaction at the Ru1 side ($|-100\ \text{cm}^{-1}/3| \approx 33\ \text{cm}^{-1}$) is appreciably smaller than the zero-field splitting value (65 cm^{-1}). This may be the reason why the magnetic behavior was simulated by the equation based on the spin pair model.

The calculation based on the molecular field approximation for the system shown in Scheme 2 was made in order to estimate the interaction between the coupled $(S_1=3/2)-(S_2=1/2)$ units.[22] As exemplified by Fig. 3(D), however, the magnetic behavior of **2**·2*n*(benzene) cannot be simulated by the equation for the system (Scheme 2) when J' has any finite

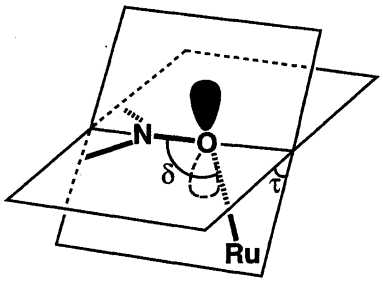

Fig. 4. Definition of the angle parameters δ and τ; δ is defined as the Ru–O–N angle, and τ the dihedral angle between the Ru–O–N plane and the nitph plane.

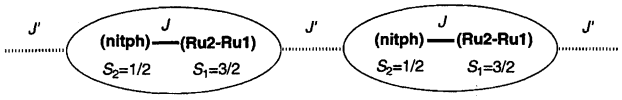

Scheme 2.

value. This result also shows that the interaction at the Ru1 side is negligibly small compared with that at the Ru2 side.

The explanation based on the difference of bonding feature between the Ru1 and Ru2 sides could not be sufficient for the result that the antiferromagnetic interactions between the Ru(II,III) core and the nitroxide radical are considerably different between Ru1 and Ru2 sides. However, it is certain that the zero-field splitting within the Ru(II,III) core plays an important role in the magnetic behavior of **2**·2*n*(benzene). In order to attain the ferrimagnetism in the combination of the Ru(II,III) dimer and the nitroxide bridging ligand, it is necessary to introduce enough interaction between the dimer and the radical to overcome the zero-field splitting within the dimer.

Appendix

Spin Pair Model of $S_1 = 3/2$ and $S_2 = 1/2$. The theoretical magnetic susceptibility of the spin pair of $S_1 = 3/2$ and $S_2 = 1/2$ is calculated using the Van Vleck formula. The Hamiltonian is

$$\mathcal{H} = \mathcal{H}_0 + \mu_B(g_1\vec{S}_1 + g_2\vec{S}_2)\vec{H},$$

with

$$\mathcal{H}_0 = -2J\vec{S}_1\cdot\vec{S}_2 + D[S_{1z}^2 - \frac{1}{3}S_1(S_1+1)],$$

Table 5. Overlap Integral between the π^* Orbitals[a] of the Ru_2 Core[21] and the π^* Orbital[a] of the Oxygen Atom of the Nitroxide Radical in **2**·2*n*(benzene)

	M–O_{ax}/Å	δ[b]/°	τ[b]/°	$\theta_{i,j}$[c]/°	Overlap integral $\mathcal{S}_{i,j}$[d]	$\mathcal{S}_{Rui}^2 = \mathcal{S}_{i,1}^2 + \mathcal{S}_{i,2}^2$
Ru1–O_{ax}	2.264	131.7	81	$\theta_{1,1}=46$, $\theta_{1,2}=44$	$\mathcal{S}_{1,1}=9.77\times10^{-3}$, $\mathcal{S}_{1,2}=7.51\times10^{-3}$	$\mathcal{S}_{Ru1}=1.52\times10^{-4}$
Ru2–O_{ax}	2.236	147.5	38	$\theta_{2,1}=84$, $\theta_{2,1}=8$	$\mathcal{S}_{1,2}=1.83\times10^{-2}$, $\mathcal{S}_{2,2}=1.07\times10^{-2}$	$\mathcal{S}_{Ru2}=4.49\times10^{-4}$

a) The π^* orbitals are assumed to be the 4d orbitalds of the ruthenium atom and the 2p orbital of the oxygen atom with the effective nuclear charges of 14 and 4, respectively, which are smaller than the real nuclear charges of 44 and 8 due to the screening effect by the core electrons. b) The angle parameters δ and τ are defined in Fig. 4 c) The parameter $\theta_{1,1}$ is defined by the mean value of the dihedral angles between the plane Ru1–O9–N1 and the plane Ru1–Ru2–O1 and between the plane Ru1–O9–N1 and the plane Ru1–Ru2–O5. The other parameters $\theta_{1,2}$, $\theta_{2,1}$ and $\theta_{2,2}$ are defined in this manner. d) $\mathcal{S}_{i,1}$ and $\mathcal{S}_{i,2}$ ($i=1,2$) are the overlap integrals of the $d_{x'z'}$ and $d_{y'z'}$ orbitals of the ruthenium atom with the p_z orbital of the oxygen atom, the z′ axis being in the direction of the Ru→O_{ax} vector.

where $\vec{H}$ is the applied magnetic field, and D is the axial zero-field splitting parameter for the $\vec{S}_1$.

The total spin is defined as

$$\vec{S} = \vec{S}_1 + \vec{S}_2.$$

Using the representation $|S,S_Z\rangle$, the eigenvalues and the eigenstates of the unperturbed Hamiltonian $\mathscr{H}_0$ become as follows:

eigenvalues of $\mathscr{H}_0$	eigenstates
$E_1 = -\frac{3}{2}J + D$	$\begin{cases} \|2,2\rangle \\ \|2,-2\rangle \end{cases}$
$E_2 = -\frac{3}{2}J - D$	$\|2,0\rangle$
$E_3 = \frac{5}{2}J - D$	$\|1,0\rangle$
$E_4 = \frac{1}{2}J + \delta$	$\begin{cases} \cos\theta_+\|2,1\rangle + \sin\theta_+\|1,1\rangle \\ \cos\theta_+\|2,-1\rangle - \sin\theta_+\|1,-1\rangle \end{cases}$
$E_5 = \frac{1}{2}J - \delta$	$\begin{cases} \cos\theta_-\|2,1\rangle + \sin\theta_-\|1,1\rangle \\ \|\cos\theta_-\|2,-1\rangle - \sin\theta_-\|1,-1\rangle \end{cases}$

where

$$\delta = \sqrt{4J^2 + 2DJ + D^2},$$

and

$$\tan\theta_\pm = \frac{2J + \frac{1}{2}D \pm \delta}{\frac{\sqrt{3}}{2}D}.$$

Then, the susceptibility of the powder sample is calculated using the Van Vleck formula. The result is as follows:

$$\begin{aligned}
\chi &= \frac{1}{3}(\chi_{//} + 2\chi_\perp) \\
&= \frac{N\mu_B^2}{3kT}\frac{1}{Z}\left[Ae^{-E_1/kT} + P_+e^{-E_4/kT} + P_-e^{-E_5/kT}\right. \\
&\quad -2kT\left\{\left(\frac{Q_+}{E_1-E_4} + \frac{Q_-}{E_1-E_5}\right)e^{-E_1/kT}\right. \\
&\quad + \left(\frac{B}{E_2-E_3} + \frac{R_+}{E_2-E_4} + \frac{R_-}{E_2-E_5}\right)e^{-E_2/kT} \\
&\quad + \left(\frac{B}{E_3-E_2} + \frac{S_+}{E_3-E_4} + \frac{S_-}{E_3-E_5}\right)e^{-E_3/kT} \\
&\quad + \left(\frac{Q_+}{E_4-E_1} + \frac{R_+}{E_4-E_2} + \frac{S_+}{E_4-E_3} + \frac{C}{E_4-E_5}\right)e^{-E_4/kT} \\
&\quad \left.\left. + \left(\frac{Q_-}{E_5-E_1} + \frac{R_-}{E_5-E_2} + \frac{S_-}{E_5-E_3} + \frac{C}{E_5-E_4}\right)e^{-E_5/kT}\right\}\right],
\end{aligned}$$

where

$$Z = \sum_{i=1}^{5} n_i e^{-E_i/kT},$$

n_i being the multiplicity of the level E_i, and

$$A = 2\left(\frac{3}{2}g_1 + \frac{1}{2}g_2\right)^2,$$

$$B = \left(\frac{1}{2}g_1 - \frac{1}{2}g_2\right)^2,$$

$$\begin{aligned}
C = 2\left[\cos\theta_+\cos\theta_-\left(\frac{3}{4}g_1 + \frac{1}{4}g_2\right) + \sin\theta_+\sin\theta_-\left(\frac{5}{4}g_1 - \frac{1}{4}g_2\right)\right. \\
\left. +(\cos\theta_+\sin\theta_- + \sin\theta_+\cos\theta_-)\left(\frac{\sqrt{3}}{4}g_1 - \frac{\sqrt{3}}{4}g_2\right)\right]^2,
\end{aligned}$$

$$\begin{aligned}
P_\pm = 2\left[\cos^2\theta_\pm\left(\frac{3}{4}g_1 + \frac{1}{4}g_2\right) + \sin^2\theta_\pm\left(\frac{5}{4}g_1 - \frac{1}{4}g_2\right)\right. \\
\left. +2\cos\theta_\pm\sin\theta_\pm\left(\frac{\sqrt{3}}{4}g_1 - \frac{\sqrt{3}}{4}g_2\right)\right]^2,
\end{aligned}$$

$$Q_\pm = 4\left[\cos\theta_\pm\left(\frac{3}{4}g_1 + \frac{1}{4}g_2\right) + \sin\theta_\pm\left(-\frac{\sqrt{3}}{4}g_1 + \frac{\sqrt{3}}{4}g_2\right)\right]^2,$$

$$R_\pm = 4\left[\cos\theta_\pm\left(\frac{3\sqrt{6}}{8}g_1 + \frac{\sqrt{6}}{8}g_2\right) + \sin\theta_\pm\left(\frac{\sqrt{2}}{8}g_1 - \frac{\sqrt{2}}{8}g_2\right)\right]^2,$$

$$S_\pm = 4\left[\cos\theta_\pm\left(-\frac{\sqrt{6}}{8}g_1 + \frac{\sqrt{6}}{8}g_2\right) + \sin\theta_\pm\left(\frac{5\sqrt{2}}{8}g_1 - \frac{\sqrt{2}}{8}g_2\right)\right]^2.$$

The present work was partially supported by a Grant-in-Aid for Scientific Research Nos. 08404046 and 09874136 from the Ministry of Education, Science, Sports and Culture and by a grant from the Electric Technology Research Foundation of Chugoku.

References

1) J. F. Villa and W. E. Hatfield, *J. Am. Chem. Soc.*, **93**, 4081 (1971); R. C. E. Belford, D. E. Fenton, and M. R. Truter, *J. Chem. Soc., Dalton Trans.*, **1974**, 17; B. Morosin, R. C. Hughes, and Z. G. Soos, *Acta Crystallogr., Sect. B*, **31B**, 762 (1975); F. Kubel and J. Strähle, *Z. Naturforsh., B*, **38B**, 258 (1983); C. Marzin, G. Tarrago, I. Zidane, E. Bienvenue, P. Seta, C. Andrieux, H. Gampp, and J. M. Savéant, *Inorg. Chem.*, **25**, 1778 (1986); J. P. Collman, J. T. McDevitt, C. R. Leidner, G. T. Yee, J. B. Torrance, and W. A. Little, *J. Am. Chem. Soc.*, **109**, 4606 (1987); S. Knecht, R. Polley, and M. Hanack, *Appl.Organomet. Chem.*, **10**, 649 (1996).

2) a) F. A. Cotton, Y. Kim, and T. Ren, *Inorg. Chem.*, **31**, 2723 (1992); b) F. D. Cukiernik, A.-M. Giroud-Godquin, P. Maldivi, and J.-C. Marchon, *Inorg. Chim. Acta*, **215**, 203 (1994).

3) A. Caneschi, D. Gatteschi, R. Sessoli, and P. Rey, *Acc. Chem. Res.*, **22**, 392 (1989); A. Caneschi, D. Gatteschi, and P. Rey, *Prog. Inorg. Chem.*, **39**, 331 (1991); P. Rey, D. Luneau, and A. Cogne, in "Magnetic Molecular Materials," ed by D. Gatteschi, O. Kahn, J. S. Miller, and F. Palacio, Kluwer Academic Publishers, Dordrecht, Boston, and London (1991), p. 203; H. O. Stumpf, L. Ouahab, Y. Pei, P. Bergerat, and O. Kahn, *J. Am. Chem. Soc.*, **116**, 3866 (1994).

4) a) A. Cogne, A. Grand, P. Rey, and R. Subra, *J. Am. Chem. Soc.*, **109**, 7927 (1987); b) A. Cogne, A. Grand, P. Rey, and R. Subra, *J. Am. Chem. Soc.*, **111**, 3230 (1989).

5) J. S. Miller, J. C. Calabrese, R. S. McLean, and A. J. Epstein, *Adv. Mater.*, **4**, 498 (1992); J. S. Miller, C. Vazquez, N. L. Jones, R. S. McLean, and A. J. Epstein, *J. Mater. Chem.*, **5**, 707 (1995); A. Böhm, C. Vazquez, R. S. McLean, J. C. Calabrese, S. E. Kalm, J. L. Manson, A. J. Epstein, and J. S. Miller, *Inorg. Chem.*, **35**, 3083 (1996); A. J. Epstein and J. S. Miller, *Synth. Met.*, **80**, 231 (1996).

6) F. A. Cotton and Y. Kim, *J. Am. Chem. Soc.*, **115**, 8511 (1993); F. A. Cotton, Y. Kim, and J. Lu, *Inorg. Chim. Acta*, **221**, 1 (1994); X. Ouyang, C. Campana, and K. R. Dunbar, *Inorg. Chem.*, **35**, 7188 (1996); C. Campana, K. R. Dunbar, and X. Ouyang, *J. Chem. Soc., Chem. Commn.*, **1996**, 2427.

7) a) M. Handa, K. Kasamatsu, K. Kasuga, M. Mikuriya, and T. Fujii, *Chem. Lett.*, **1990**, 1753; b) M. Handa, H. Sono, K. Kasamatsu, K. Kasuga, M. Mikuriya, and S. Ikenoue, *Chem. Lett.*, **1992**, 453; c) M. Hanada, A. Takata, T. Nakao, K. Kasuga, M. Mikuriya, and T. Kotera, *Chem. Lett.*, **1992**, 2085; d) M. Handa, K. Yamada, T. Nakao, K. Kasuga, M. Mikuriya, and T. Kotera, *Chem. Lett.*, **1993**, 1969; e) M. Handa, M. Mikuriya, R. Nukada, H. Matsumoto, and K. Kasuga, *Bull. Chem. Soc. Jpn.*, **67**, 3125 (1994); f) M. Mikuriya, R. Nukada, H. Morishita, and M. Handa, *Chem. Lett.*, **1995**, 617; g) M. Handa, M. Mikuriya, T. Kotera, K. Yamada,

T. Nakao, H. Matsumoto, and K. Kasuga, *Bull. Chem. Soc. Jpn.*, **68**, 2567 (1995); h) M. Handa, H. Matsumoto, T. Namura, T. Nagaoka, K. Kasuga, M. Mikuriya, T. Kotera, and R. Nukada, *Chem. Lett.*, **1995**, 903; i) M. Handa, Y. Sayama, M. Mikuriya, R. Nukada, I. Hiromitsu, and K. Kasuga, *Chem. Lett.*, **1996**, 201; j) M. Handa, M. Mikuriya, Y. Sato, T. Kotera, R. Nukada, D. Yashioka, and K. Kasuga, *Bull. Chem. Soc. Jpn.*, **69**, 3483 (1996).

8) O. Kahn, "Molecular Magnetism," VCH Publishers (1993).

9) M. Handa, Y. Sayama, M. Mikuriya, R. Nukada, I. Hiromitsu, and K. Kasuga, *Bull. Chem. Soc. Jpn.*, **68**, 1647 (1995).

10) A. Cogne, E. Belorizky, J. Laugier, and P. Rey, *Inorg. Chem.*, **33**, 3364 (1994).

11) M. C. Barral, R. Jiménez-Aparicio, J. L. Priego, E. C. Royer, E. Gutiérrez-Puebla, and C. Ruíz-Valero, *Polyhedron*, **11**, 2209 (1992).

12) N. F. Curtis, *J. Chem. Soc.*, **1961**, 3147.

13) F. E. Mabbs and D. J. Machin, "Magnetism and Transition Metal Complexes," Chapman and Hall, London (1973).

14) C. K. Fair, "MolEN Structure Determination System," Delft Instrument, Delft, The Netherlands (1990).

15) F. A. Cotton and R. A. Walton, "Multiple Bonds between Metal Atoms," 2nd ed, Oxford Univ. Press, New York (1993), p. 399.

16) W. Wong and S. F. Watkins, *J. Chem. Soc., Chem. Commun.*, **1973**, 888; A. Grand, P. Rey, R. Subra, V. Barone, and C. Minichino, *J. Phys. Chem.*, **95**, 9238 (1991); F. L. Panthou, D. Luneau, J. Laugier, and P. Rey, *J. Am. Chem. Soc.*, **115**, 9095 (1993); A. Zheludev, V. Barone, M. Bonnet, B. Delley, A. Grand, E. Ressouche, P. Rey, R. Subra, and J. Schweizer, *J. Am. Chem. Soc.*, **116**, 2019 (1994).

17) A. Caneshchi, L. Laugier, and P. Rey, *J. Chem. Soc., Perkin Trans. 1*, **1987**, 1077.

18) The theoretical equation based on the Hamiltonian

$$\mathscr{H} = -J\sum_i \vec{S}_{2i}[(1+\alpha)\vec{S}_{1i} + (1-\alpha)\vec{S}_{1,i+1}],$$

where $(1+\alpha)J$ and $(1-\alpha)J$ represent the alternated coupling constants between $S_1=3/2$ and $S_2=1/2$ centers, respectively, was used for the analysis; see p. 281 of Ref. 8.

19) J. Telser and R. S. Drago, *Inorg. Chem.*, **23**, 3114 (1984); J. Telser, V. M. Miskowski, R. S. Drago, and N. M. Wong, *Inorg. Chem.*, **24**, 4765 (1985).

20) T. R. Felthouse, T.-Y. Dong, D. N. Hendrickson, H.-S. Shieh, and M. R. Thompson, *J. Am. Chem. Soc.*, **108**, 8201 (1986).

21) The δ^* orbital of Ru(II,III) dimer was not included in the calculation because the orbital is not spread into the space suitable for the overlap with the π^* orbital of the nitroxide radical.

22) C. J. O'Connor, *Prog. Inorg. Chem.*, **29**, 203 (1982); The equation is given by $\chi' = \frac{\chi}{1-(2zJ'/Ng^2\mu_B^2)\chi}$, where zJ' is the exchange energy J' multiplied by the number z of interacting neighbors and χ the magnetic susceptibility of the coupled $(S_1=3/2)-(S_2=1/2)$ unit appearing in Appendix.